Zernike-type phase-contrast hard X-ray microscope with a zone plate at the Photon Factory

Hiroki Yokosuka,[a] Norio Watanabe,[a]* Takuji Ohigashi,[a] Yasutoshi Yoshida,[a] Shunichi Maeda,[a] Sadao Aoki,[a] Yoshio Suzuki,[b] Akihisa Takeuchi[b] and Hidekazu Takano[b]

[a]Institute of Applied Physics, University of Tsukuba, 1-1-1 Tennoudai, Tsukuba, Ibaraki 305-8573, Japan, and [b]SPring-8, Mikazuki, Sayo-gun, Hyogo 679-5198, Japan. E-mail: watanabe@bk.tsukuba.ac.jp

A Zernike-type phase-contrast X-ray microscope with a zone plate and a phase plate was constructed at the Photon Factory BL3C2. Parallel monochromatic X-rays of 8.97 keV were incident on a specimen and a direct beam transmitted through the specimen was focused on the back focal plane of the zone plate, where an aluminium phase plate was placed. Tantalum line patterns as fine as 0.3 μm could be imaged. Phase-contrast images of polypropylene wires and polystyrene latex beads were obtained, which showed better contrast than that of their bright field images.

Keywords: phase contrast; hard X-rays; X-ray microscopes; zone plates.

1. Introduction

In the X-ray region, phase contrast is much higher than absorption contrast especially for specimens which consist of light elements, such as biological specimens. Phase-contrast imaging offers observation methods of a specimen that is almost transparent for X-rays. In the X-ray region above several keV, phase-sensitive imaging, such as phase-contrast tomography (Momose *et al.*, 1996), projection methods with partially coherent X-ray sources (Snigirev *et al.*, 1995; Wilkins *et al.*, 1996) and a defocus method with coherent illumination (Snigirev *et al.*, 1997), has been developed.

In an optical phase-contrast microscope, a phase shift of transmitted rays through a specimen is converted to an amplitude variation by a phase plate (Bennett *et al.*, 1951). Such a so-called Zernike-type phase-contrast microscope system is also suitable for X-ray imaging with high resolution. Schmahl and his collaborators developed the similar phase-contrast soft X-ray microscope with zone plates and a phase plate (Schmahl *et al.*, 1995). We developed a phase-contrast X-ray microscope with a Wolter mirror and a phase plate located at the back focal plane of the mirror (Watanabe *et al.*, 2000). However, only one-dimensional phase-contrast images could be obtained because of the figure error of the mirror.

A zone plate is a circular diffraction grating with radially increasing line density. At present, the resolution of a zone plate is much higher than that of a Wolter mirror. Using a zone plate, several X-ray full-field microscopes with submicrometre spatial resolution have been reported (Kaulich *et al.*, 1999; Leitenberger *et al.*, 2000; Kagoshima *et al.*, 2000).

In this experiment, a zone plate was used as an objective instead of the mirror to obtain phase-contrast images with higher resolution.

2. Optical system

The objective zone plate was fabricated by NTT Advanced Technology (Suzuki *et al.*, 2001). The specifications of the zone plate were the following: diameter, 100 μm; outermost zone width, 0.25 μm; number of zones, 100; pattern material, Ta; pattern thickness, 1 μm; substrate, SiN 2.4 μm thickness; Au central stop, 50 μm in diameter and 2.3 μm in thickness; focal length of 180 mm at 9 keV. The diffraction efficiency of the first order at 9 keV was about 18%.

Fig. 1 shows a schematic of the optical system of the phase-contrast microscope. The microscope was constructed at BL3C2, Photon Factory, Japan. The storage-ring energy is 2.5 GeV and the maximum ring current is about 400 mA. The white beam from the bending-magnet source was monochromated with an Si(111) double-crystal monochromator. An X-ray energy of 8.97 keV was selected, which is slightly below the copper absorption edge. The beam size was restricted to 100 μm in diameter by a pinhole in front of the specimen. Parallel monochromatic X-rays were incident on the specimen. The X-ray image was focused onto a detector by the zone plate. The magnification ratio was 10. The zone plate was set off the optical axis to prevent minus first- and zero-order X-rays from reaching the image area. A CCD camera (Hamamatsu C4880, CCD: Texas Instruments TC-215, pixel size: 12 μm) and nuclear emulsion plates (Fuji EM G-OC 15) were used as the detector. Using the CCD camera, the resolution was poorer than about 1 μm because of the low magnification ratio. Nuclear emulsion plates were used for imaging with high resolution. A gold wire of diameter 250 μm was used as a direct beam stop. These optical elements and specimen were set in air and the optical path between the phase plate and the direct beam stop was replaced with helium.

A phase plate was placed at the back focal plane of the zone plate. Undeviated X-rays through the specimen were focused at the plane, but deviated X-rays by scattering or diffraction were not focused at the plane. Thus, a phase difference could be applied to the undeviated X-rays by a phase plate located at the back focal plane. Two types of phase plate were considered. One was a point-like phase plate, which affected only undeviated X-rays. Another was a pinhole-like phase plate, which affected only deviated X-rays. Fig. 2 shows theoretical calculations of the corresponding image contrast. The specimen is supposed to be an ideal phase object that has no absorption and a

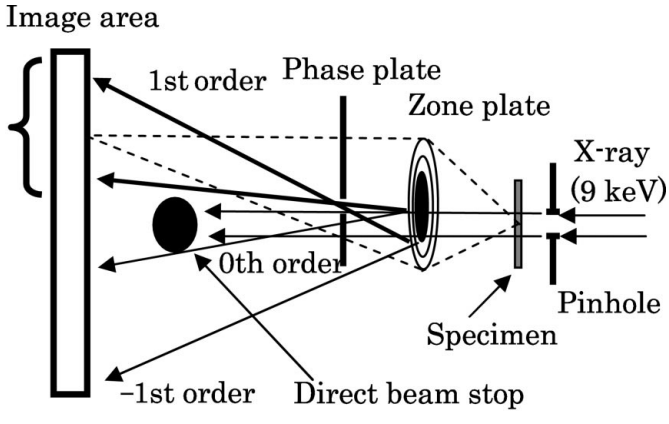

Figure 1
Schematic of the phase-contrast X-ray microscope. The zone plate was set off the optical axis to prevent minus first- and zeroth-order X-rays from reaching the image area. The image of a specimen was focused onto a CCD camera with a magnification ratio of 10. Transmitted X-rays through a specimen were focused onto the back focal plane of the zone plate, where a phase plate was placed.

phase shift of 0.01 wavelength. It is supposed that undeviated or deviated X-rays are advanced by a quarter-wavelength in phase by the respective phase plate. The calculation method was that followed by Bennett *et al.* (1951). Fig. 2 shows that, if the transmittance of the phase plate is less than 20%, much better contrast can be obtained in the case of the point-like phase plate. However, all materials are fairly transparent for 9 keV X-rays. In the case of a gold quarter-wavelength phase plate, the transmittance is 76% at 9 keV and the calculated contrast is not so different between these two types of phase plates. Thus, a pinhole-like aluminium quarter-wavelength phase plate was used in this experiment.

The synchrotron radiation source was located 35 m upstream of the optical system and its source size was $2.35\sigma_x = 0.68$ mm horizontally and $2.35\sigma_y = 0.20$ mm vertically (Photon Factory, 2001). The reduced source image size was calculated to be 3.5 μm horizontally and 1.0 μm vertically at the phase plate. A pinhole size larger than this source size is necessary to distinguish the undeviated and deviated X-rays. Thus, an aluminium phase plate with a pinhole of 12 μm in diameter was used. The pinhole was made by electrodischarge machining. The Al thickness was 5 μm, which corresponded to a phase shift of a quarter-wavelength and a transmittance of 96% for 8.97 keV X-rays.

Fig. 3(*a*) shows the phase plate for phase-contrast microscopy. The pinhole of the phase plate was placed at the focused point of illuminating X-rays. Undeviated X-rays through a specimen were transmitted through the pinhole, and not affected by the phase plate. However, deviated X-rays by scattering or diffraction were transmitted through the Al foil of the phase plate, and the phase was advanced by a quarter-wavelength. This corresponded to negative phase contrast. Fig. 3(*b*) shows an X-ray image without a specimen recorded on the CCD camera. The left-hand side is the real image and the right-hand side is the imaginary image corresponding to the negative first-order X-rays. The phase plate was almost transparent for 8.97 keV X-rays. However, the pinhole of the phase plate could be observed with good contrast as shown on the right-hand side of Fig. 3(*b*) because the right-hand-side image corresponded to the projection image from a demagnified source point of the synchrotron radiation and the interference contrast could be observed in the same manner as phase-contrast radiography (Wilkins *et al.*, 1996). Thus, the pinhole could be easily located at the focused point of the zone plate.

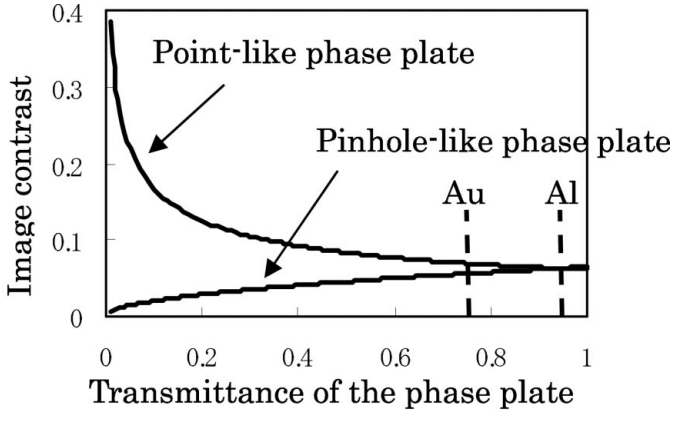

Figure 2
Absolute values of calculated image contrast of a phase object (no absorption, phase shift: 0.01 wavelength). It is assumed that the point-like phase plate decreases the optical path of undeviated X-rays by a quarter-wavelength, whereas the pinhole-like phase plate decreases deviated X-rays by a quarter-wavelength. Au and Al in the figure indicate the transmittances of the quarter-wavelength phase plate of these elements.

3. Performance test and application

The performance of the microscope was evaluated with a tantalum test pattern. The pattern has line structures with line-and-space widths from 0.1 to 1.0 μm at intervals of 0.1 μm. The pattern thickness was 0.5 μm, which corresponded to a transmittance of 91%. All X-ray images presented afterwards were recorded on nuclear emulsion plates, enlarged by an optical microscope, and displayed as photographic positive where white represented high intensity.

Fig. 4(*a*) shows the bright field image at 8.97 keV without the phase plate. This is a slightly defocused image so that the outline of the pattern can be seen (Snigirev *et al.*, 1997). A minimum horizontal line width of 0.3 μm could be resolved. Fig. 4(*b*) shows the phase-contrast image of the test pattern with the phase plate. Not only the outline of the pattern but also the internal areas of the Ta stripes could be observed as dark areas, which correspond to negative phase contrast.

Fig. 5 shows images of polypropylene fibres of diameter 7.4 μm recorded on nuclear emulsion plates. The transmittance of a 7.4 μm-thick polypropylene film is calculated to be 99.8%; consequently, this specimen can be regarded as a phase object. Fig. 5(*a*) shows the defocus bright field image without the phase plate and Fig. 5(*b*) shows the phase-contrast image with the phase plate. The outline of the fibres could be observed in the defocus condition of the bright field mode, but the phase-contrast image showed better contrast than that of the amplitude contrast image. The observed contrast of the phase-contrast image was estimated to be 0.19 from the CCD image of the same specimen, whereas the corresponding calculated contrast of the polypropylene fibers is 0.68. It is thought that the contrast degradation resulted from the relatively large pinhole size of the phase plate compared with the reduced source image size, so that the phase difference could not be applied to a fair part of the deviated X-rays from the specimen.

Observation of hydrated biological specimens is one of the most promising targets for X-ray microscopy. In order to observe hydrated biological specimens, a specimen holder that consisted of two quartz sheets of thickness 30 μm was made and tested. Polystyrene latex beads of diameter 2.8 μm were selected as a test specimen. Fig. 6(*a*) shows a schematic of the specimen holder. The polystyrene latex solution and a copper mesh of pitch 25.4 μm were sandwiched with two sheets of quartz. The spacing between the two sheets was about 100 μm. Fig. 6(*b*) shows the phase-contrast image of this at 8.97 keV. Not only the beads in the open space of the copper mesh but also the beads behind the mesh bar could be observed. The calculated image

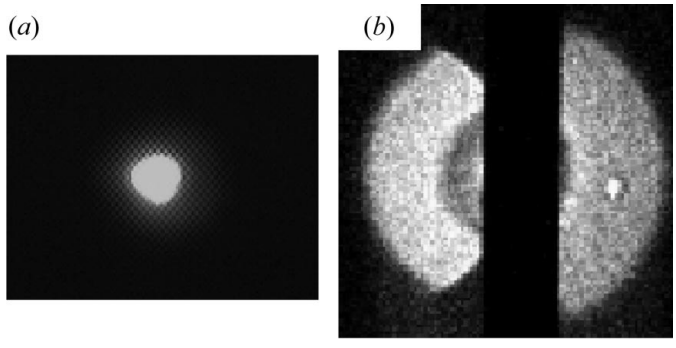

Figure 3
(*a*) Al phase plate with a pinhole of diameter 12 μm. (*b*) X-ray image without a specimen recorded on the CCD camera. The left-hand side is the real image and the right-hand side is the imaginary image corresponding to the negative first-order X-rays. The bright spot in the right-hand side is the projection of the pinhole of the phase plate.

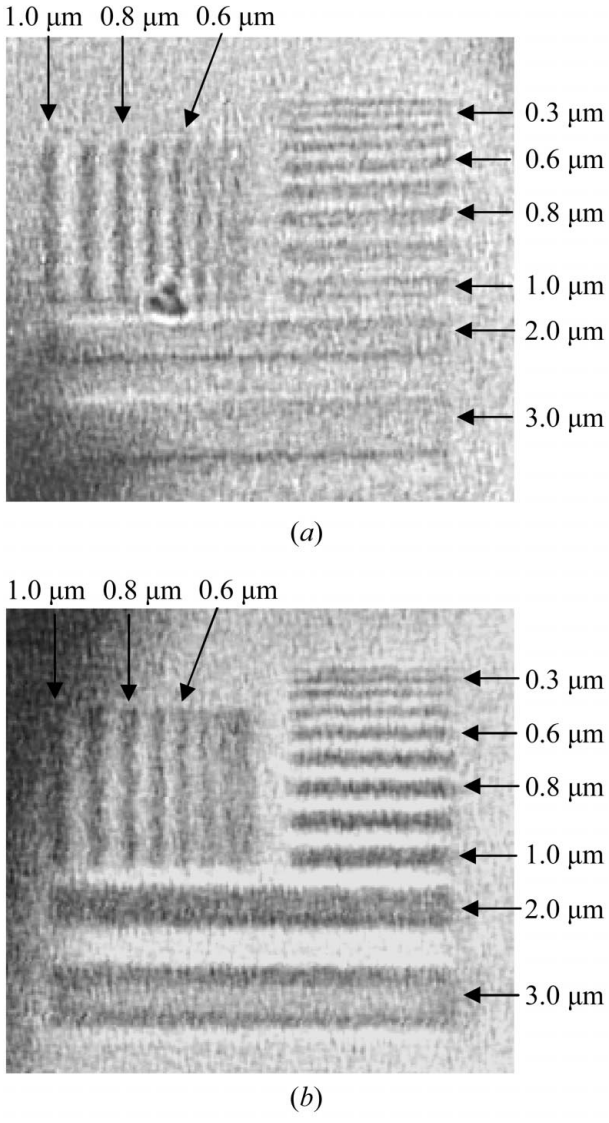

Figure 4
Bright field X-ray image (*a*) and phase-contrast image (*b*) of a Ta test pattern at 8.97 keV. The widths of the Ta lines were in the range 0.1–3.0 μm. The images were recorded on nuclear emulsion plates. The exposure time was 30 s.

contrasts of the polystyrene beads in air and in water are 0.41 and 0.0088, respectively. The image contrast of the beads in water is very low to observe. Thus, it is thought that the polystyrene latex solution was almost dried before this observation.

In conclusion, we have demonstrated a phase-contrast X-ray microscope with a zone plate and an Al phase plate at 8.97 keV. A line-and-space pattern as fine as 0.3 μm could be imaged. Almost transparent specimens, such as polypropylene fibres and polystyrene latex beads, could be observed. These specimens could be observed in the defocus bright field mode; however, the better contrast could be obtained in the phase-contrast mode with the phase plate.

We thank Professor M. Ando, X. Zhang and H. Sugiyama for their support during the experiments at the Photon Factory. This work was supported by a Grant-in-Aid for Scientific Research (B) No. 12450037 from the Ministry of Education, Culture, Sports, Science and Technology of Japan.

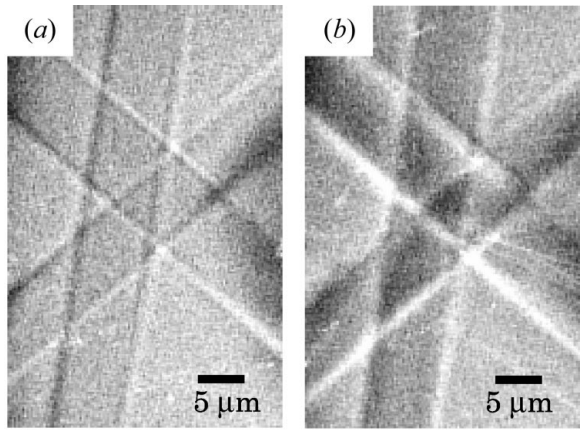

Figure 5
Bright field X-ray image (*a*) and phase-contrast image (*b*) of polypropylene fibres at 8.97 keV. The images were recorded on nuclear emulsion plates. The exposure time was 90 s.

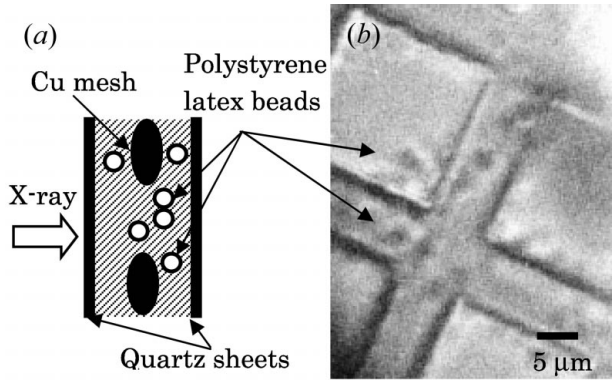

Figure 6
(*a*) Schematic of polystyrene latex beads of diameter 2.8 μm in a specimen holder. The polystyrene latex solution and a Cu mesh of pitch 25.4 μm were sandwiched with two sheets of quartz. (*b*) X-ray phase-contrast image at 8.97 keV. A nuclear emulsion plate was used. The exposure time was 90 s.

References

Bennett, A. H., Osterberg, H., Jupnik, H. & Richards, O. W. (1951). *Phase Microscopy Principles and Applications*, ch. 2. New York: John Wiley.
Kagoshima, Y., Ibuki, T., Takai, K., Yokoyama, Y., Miyamoto, N., Tsusaka, Y. & Matsui, J. (2000). *Jpn. J. Appl. Phys.* **39**, L433–L435.
Kaulich, B., Oestreich, S., Salome, M., Barrett, R. & Susini, J. (1999). *Appl. Phys. Lett.* **75**, 4061–4063.
Leitenberger, W., Weitkamp, T., Drakopoulos, M., Snigireva, I. & Snigirev, A. (2000). *Opt. Commun.* **180**, 233–238.
Momose, A., Takeda, T., Itai, Y. & Hirano, K. (1996). *Nature Medicine*, **2**, 473–475.
Photon Factory (2001). *Photon Factory Activity Report 2000*, p. 113. Photon Factory, Tsukuba, Japan.
Schmahl, G., Rudolph, D., Guttmann, P., Schneider, G., Thieme, J. & Niemann, B. (1995). *Rev. Sci. Instrum.* **66**, 1282–1286.
Snigirev, A., Snigireva, I., Böosecke, P., Lequien, S. & Schelokov, I. (1997). *Opt. Commun.* **135**, 378–384.
Snigirev, A., Snigireva, I., Kohn, V., Kuznetsov, S. & Schelokov, I. (1995). *Rev. Sci. Instrum.* **66**, 5486–5492.
Suzuki, Y., Takeuchi, A., Takano, H., Ohigashi, T. & Takenaka, H. (2001). *Jpn. J. Appl. Phys.* **40**, 1508–1510.
Watanabe, N., Aoki, S., Takano, H., Yamamoto, K., Takeuchi, A., Tsubaki, H. & Aota, T. (2000). *X-ray Microscopy: Proceedings of the Sixth International Conference*, edited by W. Meyer-Ilse, T. Warwick & D. Attwood, pp. 84–91. New York: American Institute of Physics.
Wilkins, S. W., Gureyev, T. E., Gao, D., Pogany, A. & Stevenson, A. W. (1996). *Nature (London)*, **384**, 335–338.

Received 13 November 2001 • Accepted 4 March 2002